

## 1    **Understanding the microbial biogeography of ancient human dentitions to guide** 2    **study design and interpretation**

3

4    Zandra Fagernäs<sup>1,2</sup>, Domingo C. Salazar-García<sup>3,4,5</sup>, Azucena Avilés<sup>6</sup>, María Haber<sup>6</sup>, Amanda Henry<sup>7</sup>,  
5    Joaquín Lomba Maurandi<sup>6</sup>, Andrew Ozga<sup>8</sup>, Irina M Velsko<sup>1,2</sup>, Christina Warinner<sup>1,2,9,10</sup>

6

7    1. Department of Archaeogenetics, Max Planck Institute for the Science of Human History, Jena, Germany.  
8    2. Department of Archaeogenetics, Max Planck Institute for Evolutionary Anthropology, Leipzig, Germany.  
9    3. Departament de Prehistòria, Arqueologia i Història Antiga, Universitat de València, València, Spain.  
10    4. Grupo de Investigación en Prehistoria IT-1223-19 (UPV-EHU)/IKERBASQUE-Basque Foundation for  
11    Science, Vitoria, Spain.  
12    5. Department of Geological Sciences, University of Cape Town, Cape Town, South Africa.  
13    6. Departamento de Prehistoria, Arqueología, Historia Antigua, Historia Medieval y Ciencias y Técnicas  
14    Historiográficas, Universidad de Murcia, Murcia, Spain.  
15    7. Faculty of Archaeology, Leiden University, Leiden, the Netherlands.  
16    8. Halmos College of Arts and Sciences, Nova Southeastern University, Fort Lauderdale, FL, USA.  
17    9. Faculty of Biological Sciences, Friedrich Schiller University, Jena, Germany.  
18    10. Department of Anthropology, Harvard University, Cambridge, MA, USA

19

### 20    **Abstract**

21    The oral cavity is a heterogeneous environment, varying in factors such as pH, oxygen levels, and  
22    salivary flow. These factors affect the microbial community composition and distribution of species in  
23    dental plaque, but it is not known how well these patterns are reflected in archaeological dental calculus.  
24    In most archaeological studies, a single sample of dental calculus is studied per individual and is  
25    assumed to represent the entire oral cavity. However, it is not known if this sampling strategy introduces  
26    biases into studies of the ancient oral microbiome. Here, we present the results of a shotgun  
27    metagenomic study of a dense sampling of dental calculus from four Chalcolithic individuals from the  
28    southeast Iberian peninsula (ca. 4500-5000 BP). Inter-individual differences in microbial composition are  
29    found to be much larger than intra-individual differences, indicating that a single sample can indeed  
30    represent an individual in most cases. However, there are minor spatial patterns in species distribution  
31    within the oral cavity that should be taken into account when designing a study or interpreting results.  
32    Finally, we show that plant DNA identified in the samples may be of environmental origin, showing the  
33    importance of including environmental controls or several lines of biomolecular evidence.

34

35 **Introduction**

36 Dental calculus forms when the dental plaque biofilm mineralizes during life (Jin and Yip 2002), a periodic  
37 occurrence that encapsulates microbes, host biomolecules, food residues, and particles from the  
38 environment (Velsko and Warinner 2017). After the death of an individual, biomolecules within dental  
39 calculus can be preserved for tens of thousands of years (Fellows Yates *et al.* 2021), largely protected  
40 from environmental processes within the mineral matrix. Studies of archaeological dental calculus have  
41 rapidly increased in number in recent years, in part due to an elevated interest in the evolution of the oral  
42 microbiome and a growing understanding of the plethora of ancient biomolecules and information that can  
43 be recovered from this semi-fossilized microbial biofilm. However, there are still many unknown factors  
44 regarding the formation and preservation of archaeological dental calculus, and further method  
45 development is therefore necessary.

46 In carrying out comparative studies of ancient dental calculus, researchers aim to set up a sampling  
47 strategy that mitigates biases caused by intra-individual variability of the studied individuals. However, as  
48 archaeological dental calculus is often found in small quantities, especially in individuals dating far back in  
49 time, and is not always present on the same teeth across individuals, it may not always be possible to  
50 adhere to such a sampling scheme. Pre- and post-mortem tooth loss can further complicate sampling  
51 designs, as does working with calculus samples that were dislocated from the teeth during handling or  
52 storage, such that the precise tooth of origin is unknown. Due to such sampling constraints, some studies  
53 have pooled and homogenized calculus from several teeth for analysis (Warinner *et al.* 2014), which may  
54 partly mitigate spatial biases, but this approach requires the presence and collection of larger amounts of  
55 calculus, which is a finite archaeological substrate. In light of these challenges, most ancient oral  
56 microbiome studies implicitly assume that a single sample can be representative of the entire dentition,  
57 regardless of the tooth niche from which the calculus sample is obtained, and analyze only a single dental  
58 calculus deposit per individual. The oral cavity, however, is not a uniform environment, and thus microbial  
59 communities may vary across the dentition, potentially leading to bias when comparing across individuals  
60 from whom different teeth were sampled.

61 Differences in the microbial composition of different oral tissues, such as buccal mucosa, keratinized  
62 gingiva, saliva, and teeth, have been reported in present-day humans (Aas *et al.* 2005; Ding and Schloss  
63 2014; Eren *et al.* 2014; Mark Welch *et al.* 2016; Proctor *et al.* 2018; Utter *et al.* 2020). Further, differences  
64 in dental plaque microbial communities have been previously reported between mandibular and maxillary  
65 teeth (Haffajee *et al.* 2009; Simon-Soro and Tomás 2013), between tooth position (e.g. anterior vs.  
66 posterior teeth) (Haffajee *et al.* 2009; Proctor *et al.* 2018), between tooth surfaces (e.g. buccal vs. lingual)  
67 (Simon-Soro and Tomás 2013; Proctor *et al.* 2018), and between supragingival and subgingival plaque  
68 (Simon-Soro and Tomás 2013; Eren *et al.* 2014). Local variations in oral physiological conditions, such as  
69 salivary flow rate, salivary composition, oxygen availability, and mechanical abrasion during mastication,  
70 may contribute to these subtle spatial microbial differences in dental plaque. However, while such spatial  
71 differences have been detected in the microbial composition of dental plaque, it is not known whether  
72 these patterns are also reflected in dental calculus. Dental calculus represents a fully mature stage of oral  
73 biofilm development that is often disrupted in living individuals practicing oral hygiene, leading to a distinct  
74 microbial profile between dental plaque and dental calculus (Velsko *et al.* 2019; Kazarina *et al.* 2021).  
75 Overall, dental calculus typically contains higher proportions of late colonizer taxa that thrive in the  
76 anaerobic environment created as the biofilm matures, and thus its composition may be less spatially  
77 variable than developing plaque biofilms, which are more dynamic and subject to periodically disruptive  
78 forces such as toothbrushing (Velsko *et al.* 2019).

79 However, evaluating intra-individual microbial variation in dental calculus across the dental arcade, and

80 thus determining the degree to which a single sample can represent an individual, is challenging. Dense  
81 sampling of calculus is often hindered by missing teeth or a lack of calculus deposits distributed across  
82 the entire dental arcade. Consequently, previous studies have attempted to identify microbial spatial  
83 patterns across the dentition by instead sampling diverse individual teeth from a large number of  
84 individuals (Farrer *et al.* 2018), but this introduces a number of uncontrolled variables, such as individual  
85 differences, different biological and absolute ages of samples, different postmortem conditions, and  
86 differing degrees of preservation and degradation, which may introduce biases or otherwise alter the  
87 observable spatial patterns. Further, this approach does not allow for comparisons of how much of the  
88 variation in the dental calculus microbiome stems from intra- vs. inter-individual differences.

89 To determine the degree to which tooth selection matters in dental calculus sampling for comparative  
90 ancient microbiome studies, we conducted a systematic analysis of microbial spatial variation in four  
91 nearly complete human dentitions with low to heavy dental calculus deposits from the Iberian Chalcolithic  
92 site of Camino del Molino (ca. 4500-5000 BP). With dense sampling across tooth types (incisor, canine,  
93 premolar, molar) and tooth surfaces (buccal, labial, interproximal, occlusal), we performed shotgun  
94 metagenomic analysis of 87 dental calculus samples. We find that the main source of variation in the oral  
95 microbiome is the sampled individual, and therefore one randomly selected sample can, for most  
96 purposes, be used to represent an individual in population-level comparative studies. However, minor  
97 intra-individual patterns in community composition, functional potential, and species abundances are  
98 detectable with respect to tooth position (anterior vs. posterior), dental calculus deposit size, and tooth  
99 surface, although with low effect sizes. Only occlusal calculus, which is uncommon and may indicate  
100 injury or physiological dysfunction, considerably differed in composition. We found that ancient human  
101 DNA is randomly distributed across the dentition, and no spatial patterns were observed with respect to  
102 postmortem environmental contamination. Finally, we found that ancient grapevine (*Vitis vinifera*) DNA  
103 was present in the dental calculus we analyzed; however, it was also present in mandibular bone,  
104 suggesting a contaminant origin. Given that the site of Camino del Molino is located in close proximity to  
105 historic and contemporary vineyards, these findings suggest that local agricultural fields may represent a  
106 source of contamination at archaeological sites. This study contributes to an awareness of spatial  
107 variation in dental calculus microbial community composition that aims to aid researchers in developing  
108 robust study designs and valid interpretations for ancient oral microbiome studies.

109

## 110 **Materials and Methods**

### 111 *Samples*

112 Dental calculus was collected from four Chalcolithic (4500-5000 BP) individuals from the southeastern  
113 Iberian archaeological site of Camino del Molino near the city of Caravaca de la Cruz in Murcia, Spain,  
114 excavated during a salvage excavation in 2008 (Lomba Maurandi *et al.* 2009; Lomba Maurandi, López  
115 Martínez and Ramos Martínez 2009; Haber-Uriarte, Avilés-Fernández and Lomba-Maurandi 2011). The  
116 Camino del Molino communal burial is a natural pit with a 7 meter diameter circular base and a depth of 4  
117 meters (of which only the lower 2 meters were used for burial), which was likely covered and sealed by a  
118 perishable structure (Lomba Maurandi *et al.* 2009). The upper layers of the site were destroyed in the  
119 early 20<sup>th</sup> century as a result of agricultural terracing, but the damage did not extend to the burial  
120 deposits. Approximately 1,300 human individuals representing a broad demographic profile were buried  
121 at the site between 2800-2400 BCE (Haber-Uriarte, Avilés-Fernández and Lomba-Maurandi 2011). The  
122 site was chosen for this study because prior dental calculus research at the site had shown excellent oral  
123 microbiome preservation (Ziesemer *et al.* 2015; Mann *et al.* 2018), and microfossil studies of the dental

124 calculus had been conducted (Power *et al.* 2014), and because the large number of individuals excavated  
125 from the site made it possible to select suitable individuals with nearly complete dentitions and sufficient  
126 dental calculus for this study. The four selected individuals were adults and had dental calculus present  
127 on most teeth (Figure 1, S1), allowing near comprehensive sampling. Dental notation below follows the  
128 FDI World Dental Federation standard (Peck and Peck 1993); molar enamel wear is reported as a  
129 Brothwell score from 1 (none) to 7 (obliteration of crown and wear of roots) (Brothwell 1972), and dental  
130 calculus deposits are graded from 1 (slight) to 4 (gross) according to Dobney and Brothwell (1987).

131 Individual CM55. Individual CM55 (35-39 year old female) had a complete mandible and a partial,  
132 fragmented maxilla, with a total of 22 teeth (Figure 1). Alveolar bone loss and reactive bone formation  
133 was observed throughout the mandibular periodontium, suggesting generalized periodontitis. Gross  
134 carious lesions were present in teeth 17, 35, 37, 45, and 47. Molar enamel wear was low (Brothwell stage  
135 2). Dental calculus deposits were grade 1-2 in size, except on left premolars and molars, where they  
136 reached grade 4. The excessive calculus accumulation on the left posterior teeth, including on the  
137 occlusal surfaces, suggests that this individual had experienced pain on the left side of the mouth and  
138 avoided mastication on this side. Although no skeletal trauma was apparent, CM55 had experienced  
139 antemortem tooth loss of teeth 36 and 38, and a large carious lesion was present in 37. Significant  
140 alveolar recession and reactive bone formation was also evident around 24, but damage to the left  
141 maxilla prohibited further inspection of the bone supporting the upper molar teeth.

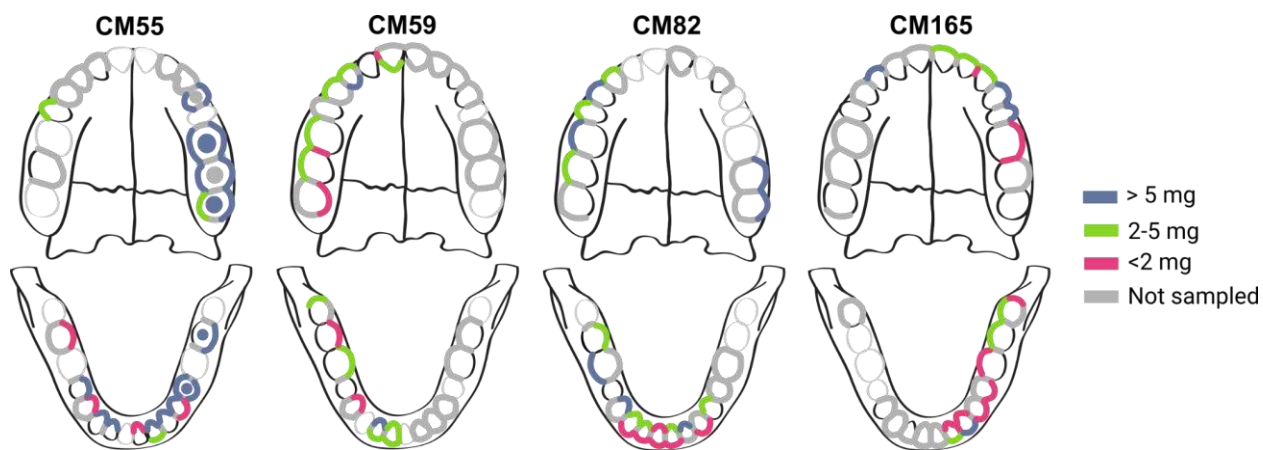
142 Individual CM59. Individual CM59 (25-35 year old male) had an intact mandible and a partial, fragmented  
143 maxilla, with a total of 25 teeth (Figure 1). Molar enamel wear was minimal (Brothwell stage 1-2), and no  
144 gross carious lesions were observed. Dental calculus deposits were grade 1-2 in size. Alveolar recession  
145 was slight across the periodontium, and in general the individual exhibited good dental health.

146 Individual CM82. Individual CM82 (35-45 year old female) had a complete mandible and a partial,  
147 fragmented maxilla, with a total of 23 teeth (Figure 1). Heavy enamel wear (Brothwell stage 4) was  
148 observed on the molar teeth. Dental calculus deposits were grade 1-2 in size. A large bone abscess was  
149 present adjacent to the healed alveolar bone where teeth 37 and 38 had been lost antemortem. Alveolar  
150 recession was pronounced around the molars, and healing was incomplete for four molars that had been  
151 lost antemortem. Gross carious lesions were present in teeth 16, 18, 45 and 46.

152 Individual CM165. Individual CM165 (25-30 year old likely female) had a near complete mandible and  
153 maxilla, with a total of 29 teeth (Figure 1). Although an adult, the individual retained deciduous tooth 52  
154 and the corresponding adult tooth 12 was absent, suggesting agenesis. CM165 also had a partially  
155 impacted tooth 38. Gross carious lesions were present in teeth 37, 38, and 48. Postmortem bone  
156 breakage made the alveolar margin difficult to assess, but where observable recession was not  
157 pronounced. Molar enamel wear was low (Brothwell stage 2-3), and dental calculus deposits were grade  
158 1 in size. Overall, the individual exhibited relatively good dental health.

159 Dental calculus collection was performed in an ancient DNA cleanroom environment at the University of  
160 Oklahoma (individual CM55) and the Max Planck Institute for Human History (individuals CM59, CM82  
161 and CM165) under sterile conditions following Warinner, Velsko and Fellow Yates (2019), and  
162 supragingival dental calculus was separately collected from four different surfaces on each tooth: lingual,  
163 buccal, interproximal and occlusal. For each individual, a bone sample (approximately 50 mg) was also  
164 collected from the mandibular ramus to be used as a control for microbes characteristic of the local burial  
165 environment. As bone is mainly assumed to be free of microbes during life, in the absence of disease, the  
166 microbes identified from archaeological bone stem from the burial environment, and represent taxa that  
167 have colonized the remains, including dental calculus, postmortem. A subset of dental calculus samples

168 was selected from each individual for metagenomic analysis (Figure 1). This subsampling was performed  
169 with the aim of achieving a balanced representation of dental sites and surfaces across individuals, as  
170 well as a consistent sample mass for analysis. For all individuals, dental sites or surfaces with < 1mg of  
171 dental calculus were generally excluded from analysis. For individuals CM59, CM82, and CM165, half of  
172 the dentition was sampled (right or left, depending on completeness and calculus abundance), but  
173 samples from the paired left/right side were also included as needed to balance out the sampling scheme  
174 with respect to tooth site and sample mass; this was particularly necessary for CM82. For individual  
175 CM55, dental calculus across the entire available dentition was sampled. Although dental calculus was  
176 mostly present only on the tooth buccal and lingual surfaces, the massive calculus deposits on the left  
177 molars of CM55 enabled the analysis of occlusal calculus for this individual. In addition, eight  
178 interproximal sites in CM59 and CM165 yielded sufficient calculus for analysis and were also sampled. In  
179 total, 87 calculus samples were selected from the four individuals for metagenomic analysis  
180 (Supplementary Data 1).



181  
182 **Figure 1. Study sampling design.** Dental calculus deposits investigated in this study are highlighted and  
183 correspond to the sampled tooth surface (buccal, lingual, interproximal, occlusal). The color of the  
184 highlighting indicates the initial mass of the dental calculus deposit on the teeth that were analyzed: <2  
185 mg (pink); 2-5.0 mg (green); >5.0 mg (blue). Teeth that were present are indicated in black outline; teeth  
186 that were absent are indicated in light gray outline. Dental calculus that was present but excluded from  
187 analysis (due to sampling design or insufficient starting mass) is marked in dark gray.

#### 188 *Laboratory methods*

189 Surface contamination was reduced by UV irradiation (30 s on both sides), followed by a washing step in  
190 1 mL of 0.5 M EDTA (without incubation). DNA was extracted from the calculus and bone samples using  
191 a modified version of (Dabney *et al.* 2013) adapted for dental calculus (Mann *et al.* 2018; Aron *et al.*  
192 2020) and allowing for potential future protein extraction from the same samples (Fagernäs *et al.* 2020).  
193 Briefly, the samples were decalcified in 1 mL 0.5 M EDTA for three days, after which the cell debris pellet  
194 and 100 µl of the supernatant was frozen at -20 °C and set aside for future analyses (Fagernäs *et al.*  
195 2020). To the remaining 900 µL supernatant, proteinase K (Sigma-Aldrich) was added, and the samples  
196 were incubated at room temperature overnight. The supernatant was then mixed with binding buffer (5 M  
197 guanidine hydrochloride, 0.12 M sodium acetate, 40% isopropanol) and DNA was purified using a High  
198 Pure Viral Nucleic Acid kit (Roche Life Science) according to the manufacturer's instructions. DNA was  
199 eluted in Qiagen EB buffer, to which Tween 20 had been added to a final concentration 0.05%. DNA was  
200 quantified using a Qubit HS assay (Thermo Fisher Scientific). Extraction blanks (one per batch) were  
201 processed alongside the samples. The full extraction protocol is available at (Aron *et al.* 2020).

202 Extracted DNA was processed with a partial uracil-DNA-glycosylase treatment (Rohland *et al.* 2015; Aron,  
203 Neumann and Brandt 2020) and was prepared into double-stranded libraries with dual indexing (Meyer  
204 and Kircher 2010; Kircher, Sawyer and Meyer 2012; Stahl *et al.* 2019). Library blanks were processed  
205 alongside the samples, one per batch. The DNA libraries were shotgun sequenced on an Illumina  
206 NextSeq with 75-bp paired-end chemistry. Dental calculus samples were sequenced to a depth of  $10.1 \pm$   
207 1.4 M reads (average  $\pm$  standard deviation), bone samples to  $6.6 \pm 2.0$  M reads, and blanks to  $1.7 \pm 0.7$   
208 M reads.

209 *Data analysis*

210 Preprocessing

211 The EAGER v.1.92.56 (Peltzer *et al.* 2016) pipeline was used for preprocessing of the raw data. Adapter  
212 removal and merging of reads were performed using AdapterRemoval v. 2.3.1 (Schubert, Lindgreen and  
213 Orlando 2016). The reads were mapped to the human reference genome HG19 using BWA v. 0.7.12 (Li  
214 and Durbin 2009) with default settings (-I 32, -n 0.01), and unmapped reads were extracted with  
215 SAMtools v. 1.3 (Li *et al.* 2009) for downstream microbiome analyses. The unmapped reads were aligned  
216 to a custom RefSeq database (Fellows Yates *et al.* 2021) using MALT v. 0.4.0 (Herbig *et al.* 2016)  
217 (settings -id 85.0 -top 1 -supp 0.01). This database contains all bacterial and archaeal assemblies at  
218 scaffold/chromosome/complete levels (as of November 2018), with max 10 randomly selected genomes  
219 per species (prioritizing more complete genomes), as well as the human HG19 reference genome. A  
220 preliminary screening for eukaryotic DNA was also performed as described above, using the NCBI full nt  
221 database (as of October 2017), but the custom RefSeq database was chosen for further analyses, as it  
222 has been shown to yield a higher percentage aligned sequences for dental calculus (Fellows Yates *et al.*  
223 2021). OTU tables with summarized read counts at genus level were exported through MEGAN v. 6.17.0  
224 (Huson *et al.* 2016) (Supplementary Data 2 and 3). The R-package decontam v. 1.6.0 (Davis *et al.* 2018)  
225 was used to identify putative laboratory and environmental contaminants from OTU tables, using the  
226 prevalence method with two sets of controls (cutoff 0.8 for each): mandibular bone from the sampled  
227 individuals in this study and previously published bone samples from Bronze Age Mongolia (Jeong *et al.*  
228 2018; Fellows Yates *et al.* 2021), and laboratory extraction and library preparation blanks .

229 Preservation assessment

230 A genus-level OTU table was used as input for SourceTracker v.1.0.1 (Knights *et al.* 2011). Included were  
231 also comparative samples from published shotgun microbiome studies, including 10 non-industrialized  
232 gut samples (Obregon-Tito *et al.* 2015; Rampelli *et al.* 2015), 11 industrialized gut samples (Gevers *et al.*  
233 2012; Sankaranarayanan *et al.* 2015), 10 skin samples (Oh *et al.* 2016), 11 subgingival and 10  
234 supragingival plaque samples (Gevers *et al.* 2012), 10 archaeological bone samples (Fellows Yates *et al.*  
235 2021), 10 modern dental calculus samples (Fellows Yates *et al.* 2021) and 10 archaeological sediment  
236 samples (Slon *et al.* 2017). During the SourceTracker analysis, the samples were rarefied to 10,000  
237 reads, with a training data rarefaction of 5,000. A principal component analysis was conducted on  
238 summarized genus level read counts of all samples, blanks and sources (including an additional 9  
239 modern dental calculus samples). Multiplicative zero replacement was conducted using the R-package  
240 zCompositions v. 1.3.4 (Palarea-Albaladejo and Martín-Fernández 2015) and the data was CLR-  
241 transformed (Gloor *et al.* 2017). The non-human DNA sequences were also mapped to the *Tannerella*  
242 *forsythia* representative genome (strain 9212) using EAGER v. 1.92.38 as described above. The output  
243 from DamageProfiler v. 0.3.10 (Neukamm, Peltzer and Nieselt 2020) was used to visualize damage  
244 curves for the samples, and fragment length was extracted from the output table from EAGER.

245 Community composition

246 Analyses of community composition were conducted on the MALT taxon tables, where putative  
247 contaminants had been removed, following recommendations for compositional data (Gloor *et al.* 2017).  
248 Significant differences in community composition of samples in selected metadata groups were tested  
249 using a PERMANOVA with the R-package vegan v. 2.5.6 (Oksanen *et al.* 2019), using euclidean distance  
250 and 9999 permutations, and individuals as strata when needed. A PCA was conducted as described  
251 above. Alpha diversity was analyzed using a species-level OTU table, and Shannon Index and Inverse  
252 Simpson Index were computed using the R package microbiome v. 1.8.0 (Lahti and Shetty 2012).

253 Differential abundance

254 Differential abundance of species was calculated using Songbird v1.0.1 (Morton *et al.* 2019) (--formula  
255 "Jawbone+ToothSurface+ToothPosition+DepositMass\_scaled+Individual", --epochs 10000 and --  
256 differential-prior 0.5). Tensorboard v. 1.14.0 was used for model checking. Input was a species-level OTU  
257 table, where putative contaminants were removed. Further, taxa present in fewer than three samples per  
258 individual were removed, and thereafter taxa absent in one or more of the individuals. This stringent  
259 filtering was applied in order to avoid any potential remaining contaminants or mismatching to influence  
260 the results. Two separate analyses were conducted, one without occlusal samples, and one including  
261 occlusal samples.

262 Functional analysis

263 The functional profiles of the microbial communities were extracted from the non-human DNA sequences  
264 using HUMAN N v. 2.8.0 (Franzosa *et al.* 2018), using the CocoPhlAn nucleotide database and the  
265 UniRef90 protein database. The output was normalized to copies per million, and translated into KEGG  
266 orthologies. Gene families were analyzed, without taking into account species assignments, and putative  
267 contaminants were removed from the dataset using decontam as described above (threshold 0.5 for both  
268 blanks and bones). A PCA was conducted, and drivers of variation identified using PERMANOVA, all as  
269 described above for community composition.

270 Human reads

271 In order to investigate the amount of host human DNA in the samples, while controlling for contaminating  
272 human DNA, the raw reads were mapped to the human HG19 genome as described above, with the  
273 exception of filtering for mapping quality (-q 37). Duplicates were removed using DeDup v. 0.12.2 (Peltzer  
274 *et al.* 2016), and the reads were filtered for a PMD (post-mortem damage) score of 3 using PMDtools  
275 v.0.6 (Skoglund *et al.* 2014), thereby only retaining damaged ancient reads. This is likely an  
276 underrepresentation of the number of ancient reads, as not all DNA fragments will have damage.  
277 However, assuming a consistent rate of postmortem damage accumulation over the dental arcade, the  
278 bias will be even across all sampling sites, and the patterns of damaged reads can be assumed to also  
279 represent patterns of total endogenous human reads. It was noted that occlusal samples generally have a  
280 higher percentage damage than other samples, and were therefore excluded from this analysis, as they  
281 break the assumption of equal damage. Deposit mass was accounted for in the analysis, as a positive  
282 correlation was found between deposit mass and DNA damage.

283 Plant DNA

284 During preliminary eukaryotic screening of the dental calculus samples, it was observed that the samples

285 contain a considerable amount of DNA mapping to grapevine (*Vitis vinifera*). To further explore this  
286 pattern, the complete experimental dataset of dental calculus, mandibular bone controls, and blanks were  
287 mapped to the grapevine representative genome (GCA\_000003745.2 12X) using EAGER as described  
288 above, with mapping quality set to 37. Damage profiles, specifically cytosine to thymine (C to T)  
289 transitions typical for ancient DNA, were created using DamageProfiler v.0.3.10 (Neukamm, Peltzer and  
290 Nieselt 2020).

291 **General statistics**

292 Unless otherwise stated, data was processed in R v. 3.6.1 (R Core Team 2019), using packages  
293 tidyverse 1.3.0 (Wickham *et al.* 2019), ggpubr v.0.3.0 (Kassambara 2018), readxl v.1.3.1 (Wickham and  
294 Bryan 2019), janitor v.2.0.1 (Firke 2018), and ggeffects v.0.14.3 (Lüdecke 2018). In order to investigate  
295 patterns across the dentition, linear mixed-effects models (LME) were fitted to the variables in question  
296 using lme4 v.1.1.23 (Bates *et al.* 2015), with the individual as the random effect when required. Model  
297 selection was performed with ANOVA using lmerTest v.3.1.2 (Kuznetsova, Brockhoff and Christensen  
298 2017) and Box-Cox transformations identified using MASS v.7.3.51.4 (Venables and Ripley 2002).  
299 Explanatory variables in all tests are: jawbone (mandible/maxilla), tooth surface  
300 (lingual/buccal/interproximal/occlusal), tooth position (anterior/posterior), and mass of the original calculus  
301 deposit (scaled and centered continuous variable). Incisors and canines are treated as anterior teeth;  
302 premolars and molars were treated as posterior teeth. Unless otherwise noted, occlusal calculus, which  
303 was only obtained from a single individual, was excluded from most analyses because these samples  
304 were found to break the assumption of homogeneous distribution of variance (euclidean distances,  
305 ANOVA, p=0.001). 2D illustration of DNA yield, human DNA, and environmental contamination across the  
306 dental arcade was performed with 'ili (Protsyuk *et al.* 2018), and can be accessed at  
307 <https://tinyurl.com/eyjcs674>. All R Markdown files have been deposited at  
308 [https://github.com/ZandraFagernas/dental\\_ arcade](https://github.com/ZandraFagernas/dental_ arcade).

309

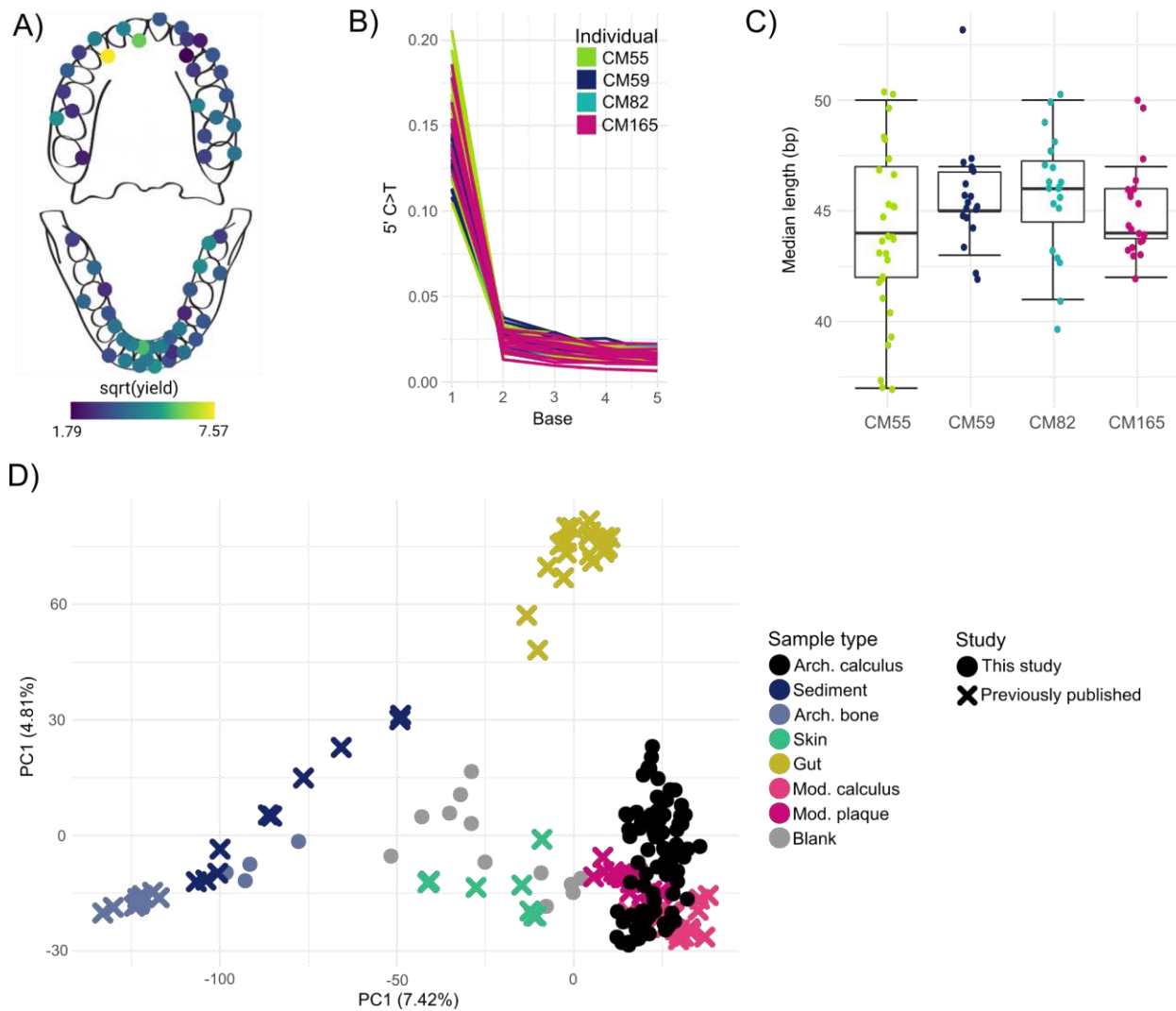
310 **Results**

311 *Preservation and authentication*

312 Total DNA yield from a sample, normalized by the mass of the dental calculus sample used for DNA  
313 extraction, may vary depending on preservation and organic matter content of the sample, and may bias  
314 downstream taxonomic profiles (Fagernäs *et al.* 2020). Occlusal samples were excluded from this  
315 analysis, as it was noted during sampling that their consistency was different from all other samples.  
316 Using linear mixed effects modeling, we tested whether tooth surface, tooth position, jawbone or deposit  
317 mass influenced the mass-normalized DNA yield from a sample. We found that none of these factors  
318 outperformed the null model (LME, individual as random effect), and therefore normalized DNA yield  
319 cannot be predicted by these variables (Figure 2A).

320 Prior to oral microbiome analysis, the archaeological dental calculus in this study was first evaluated for  
321 preservation and authenticity of the ancient oral microbiome. This is important because poor dental  
322 calculus preservation and contamination with environmental microbes can bias or interfere with  
323 downstream analyses. A PCA on genus level read counts shows that all the archaeological dental  
324 calculus samples cluster together with modern dental plaque samples, and are clearly separated from  
325 archaeological bone, gut and sediment samples (Figure 2D). To further assess preservation of the dental  
326 calculus samples, the contribution of different source environments to the composition of the samples

327 was estimated using SourceTracker (Knights *et al.* 2011). All samples were estimated to have a majority  
 328 contribution from oral microbiome sources, indicating good preservation of the oral microbiome (Figure  
 329 S2). Some samples were estimated to have a minor contribution from the skin microbiome. Minor  
 330 estimated contributions from the gut microbiome and sediment are also present, but are expected  
 331 because gut and oral taxa are similar and can be difficult to distinguish using short read data, and  
 332 because archaeological samples typically contain some soil contamination, even after washing. After  
 333 taking these factors into consideration, all dental calculus samples were determined to be sufficiently well  
 334 preserved for inclusion in downstream analyses.



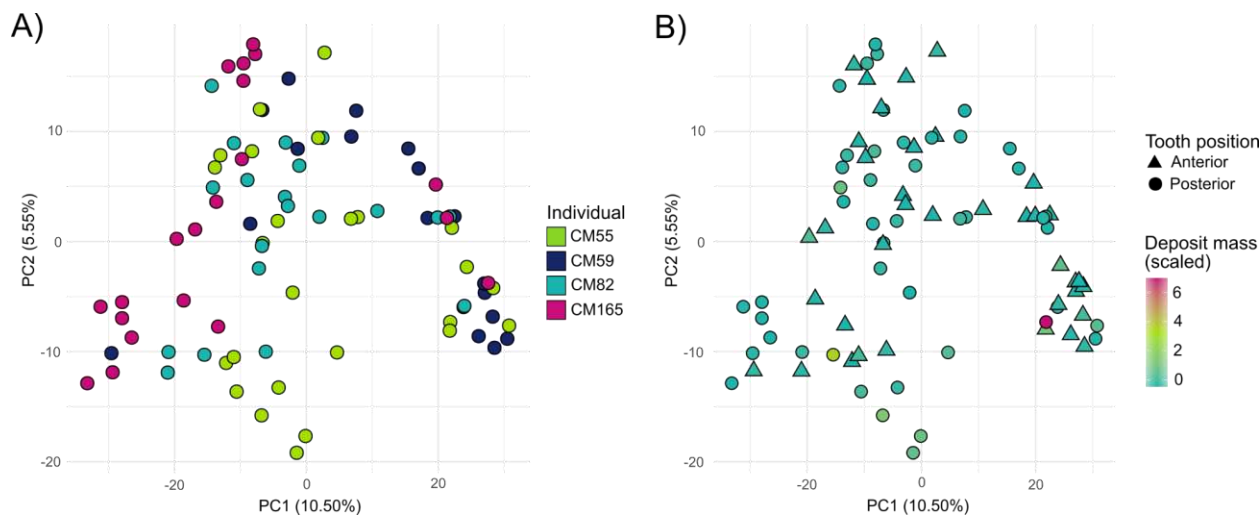
335

336 **Figure 2. Preservation assessment of dental calculus samples.** (A) normalized DNA yield (in ng DNA  
 337 per mg calculus) across the dental arcade averaged across individuals. (B) C to T transitions at the 5' end  
 338 of DNA fragments aligning to *Tannerella forsythia*, consistent with ancient DNA. Note that the sharp drop  
 339 from the first to the second base is due to treatment with uracil-DNA-glycosylase. (C) DNA aligning to *T.*  
 340 *forsythia* has short median fragment lengths, consistent with ancient DNA. (D) PCA on genus level read  
 341 counts of samples from this study, before removing putative contaminants; dental calculus from this study  
 342 forms a cluster overlapping with modern plaque and calculus, indicating good oral microbiome  
 343 preservation.

344 We next assessed DNA damage patterns in the dental calculus as an indicator of authenticity. DNA from  
345 archaeological samples accumulates specific forms of damage over time, which can be seen as C to T  
346 transitions at the ends of DNA fragments and a high degree of DNA fragmentation (Dabney, Meyer and  
347 Pääbo 2013). We generated a damage plot for fragments mapping to the prevalent oral bacterium  
348 *Tannerella forsythia* (Figure 2B), and all four individuals exhibit damage patterns typical for ancient DNA  
349 that has undergone partial UDG-treatment (Rohland *et al.* 2015). The fragment length distributions of  
350 reads mapping to *T. forsythia* show that most samples have a median length <50 bp, as is expected for  
351 ancient samples (Figure 2C). Thus, taken together, the microbial DNA present within the dental calculus  
352 of the four Chalcolithic individuals in this study is consistent with an ancient and endogenous oral  
353 microbiome.

354 *Community composition*

355 To determine whether local environmental and spatial variables along the dental arcade influence  
356 microbial community composition, we analyzed patterns of variation with the dental calculus samples.  
357 We found that the main driver of variation in a genus-level PCA was the individual from whom the sample  
358 originated (PERMANOVA,  $p<0.001$ ,  $R^2=0.14$ ; Figure 3A), indicating that the main differences in  
359 community composition are found between individuals. When controlling for the variation introduced by  
360 the individual, the mass of the calculus deposit and tooth position (anterior vs. posterior) were also found  
361 to be significant drivers of variation in community composition (PERMANOVA, individual as strata,  
362  $p=0.040$  and  $R^2=0.024$  for mass;  $p=0.021$  and  $R^2=0.032$  for tooth position; Figure 3B). However, although  
363 the differences are statistically significant in this study, when doing population-level comparisons they are  
364 unlikely to cause biases, as the  $R^2$  values are very low.



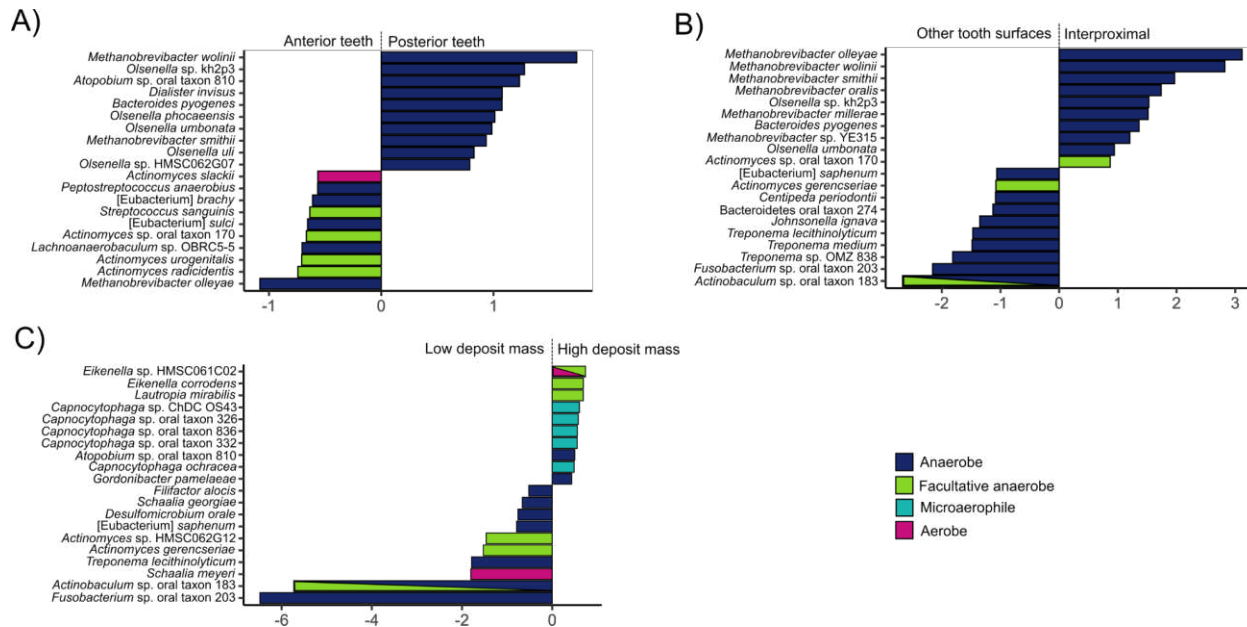
365  
366 **Figure 3. PCA on genus-level read counts.** (A) All dental calculus samples plotted together, and  
367 coloured by individual. (B) Same data as A, but with samples coloured by initial deposit mass (scaled  
368 variable) and shapes representing tooth position.

369 We next examined alpha diversity within the dataset. Alpha diversity is a measure of how rich in species  
370 the community in a certain sample is, which may be of importance when selecting samples for a  
371 community composition study. Using the inverse Simpson Index, the mass of the original calculus deposit  
372 was found to be a significant predictor of diversity in the dental calculus samples (LME, individual as  
373 random effect,  $p=0.025$ ), with diversity slightly increasing with deposit mass (Figure S3). In contrast, the  
374 null model fits the Shannon Index best, indicating that alpha diversity does not vary across the oral cavity

375 for any of the tested variables. The Simpson index takes into account evenness, and is less influenced by  
376 rare species than the Shannon Index, indicating that the generally large number of rare species in  
377 archaeological dental calculus may erode any spatial patterns in alpha diversity.

378 *Differential taxonomic abundance*

379 Due to different local environmental conditions in different areas of the oral cavity, small differences in  
380 microbial composition have been reported across the dentition in present-day dental plaque (Haffajee *et*  
381 *al.* 2009; Simon-Soro and Tomás 2013; Proctor *et al.* 2018). It is, however, not known if such patterns can  
382 be detected in archaeological samples, after both biofilm maturation during life and postmortem  
383 degradation over time. Here, we find that there are slight taxonomic differences with respect to tooth  
384 surface and initial deposit mass. First, we observe differences in taxa between anterior (incisors and  
385 canines) and posterior (premolar and molars) teeth, where the taxa that are more abundant in the anterior  
386 teeth are more often aerobic or facultatively anaerobic, while the taxa that are most associated with  
387 posterior teeth are anaerobic (Figure 4A). Second, interproximal spaces seem to be enriched in species  
388 belonging to the genera *Methanobrevibacter* and *Olsenella* (Figure 4B), which are both acid tolerant  
389 anaerobes. Finally, the species *Actinobaculum* sp. oral taxon 183 and *Fusobacterium* sp. oral taxon 203  
390 are found at a higher abundance in low mass dental calculus deposits, as compared to high mass  
391 deposits (Figure 4C). However, little is known about the physiology or role in the dental plaque biofilm of  
392 these taxa. Fusobacteria are generally secondary colonizers in the dental plaque biofilm, and bind to  
393 several other bacterial taxa (Kolenbrander 1988). A 2D model showing the spatial distributions of the taxa  
394 in Figure 4A-C across the dentition can be found at <https://tinyurl.com/eyjcs674>.

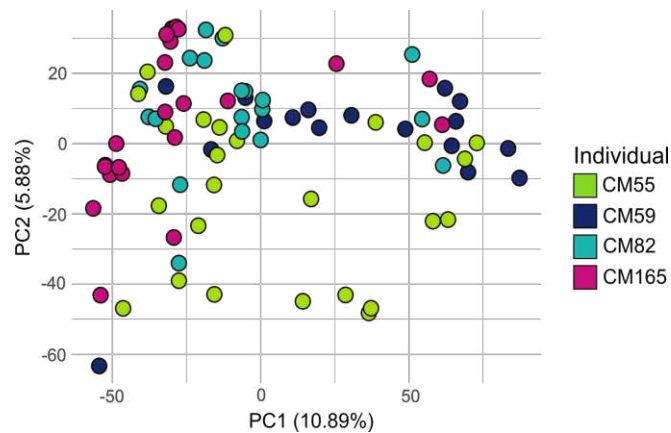


395  
396 **Figure 4. Differential abundance of species across the oral cavity.** A) Species associated with  
397 posterior (premolars and molars) vs. anterior (incisors and canines) teeth. B) Species associated with  
398 interproximal spaces vs. all other tooth sites. C) Species associated with high vs. low initial deposit mass.  
399 Only the top ten taxa most associated with each factor are shown.

400 *Functional profile*

401 In addition to their taxonomic composition, microbial communities may also differ in their gene content,

402 and therefore functional potential. It has been seen that although microbial community composition may  
403 be similar between individuals, they can differ in the functional potential of the microbiome (Fellows Yates  
404 *et al.* 2021). To evaluate whether there are potential functional differences across the dental arcade, we  
405 analyzed the genes present in the dental calculus metagenomes. In total, 2,791 gene families were  
406 identified in the dataset, after removing putative contaminants that were identified from blanks and bone  
407 samples. The individual was found to be the strongest driver of variation (PERMANOVA,  $p=0.001$  and  
408  $R^2=0.12$ ; Figure 5), and after accounting for this, tooth surface ( $p=0.020$ ,  $R^2=0.049$ ), tooth position  
409 ( $p=0.039$ ,  $R^2=0.029$ ), and deposit mass ( $p=0.013$ ,  $R^2=0.036$ ) were found to significantly drive functional  
410 variation (PERMANOVA, individual as strata). However, these factors explain only a very minor part of  
411 the variation, as can be seen by the low  $R^2$  values. It should also be noted that the tooth surface variable  
412 breaks the assumption of homogeneity of variance for this analysis, which may affect the results of the  
413 PERMANOVA.

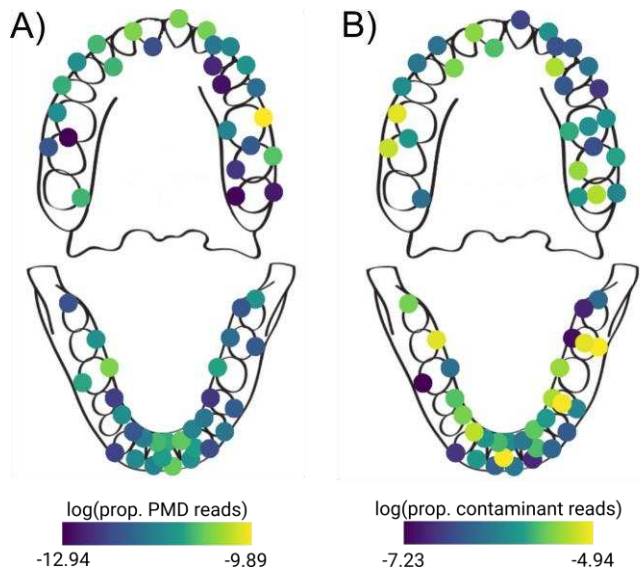


414

415 **Figure 5. Functional profile of dental calculus samples.** PCA of gene families, normalized to copies  
416 per million, with colour indicating individual.

417 *Human genetic content*

418 Although dental calculus generally contains a very low proportion of human DNA (Mann *et al.* 2018),  
419 different enrichment approaches have been used to increase the human DNA fraction enough to study  
420 the human genome (Ozga *et al.* 2016; Ziesemer *et al.* 2019). Human DNA from dental calculus is mainly  
421 derived from a single individual, the host (Ozga *et al.* 2016). Human DNA may in theory be differentially  
422 incorporated into dental calculus across the dental arcade, depending on salivary flow, inflammation, or  
423 disease, among other factors. We investigated the presence and relative abundance of ancient human  
424 DNA in our samples to assess potential spatial patterning of human host DNA in calculus. To focus our  
425 analysis on host ancient DNA, we restricted our analysis to only DNA fragments with C to T DNA  
426 damage. As a slight positive correlation was found between deposit mass and damage (Figure S4),  
427 deposit mass was accounted for in this analysis. We found that the best fitting model for predicting the  
428 proportion of human reads in the dental calculus samples is a null model, indicating that the distribution of  
429 human DNA in dental calculus does not significantly vary according to tooth surface, tooth position, or  
430 jawbone (LME, deposit mass as random effect; Figure 6A).



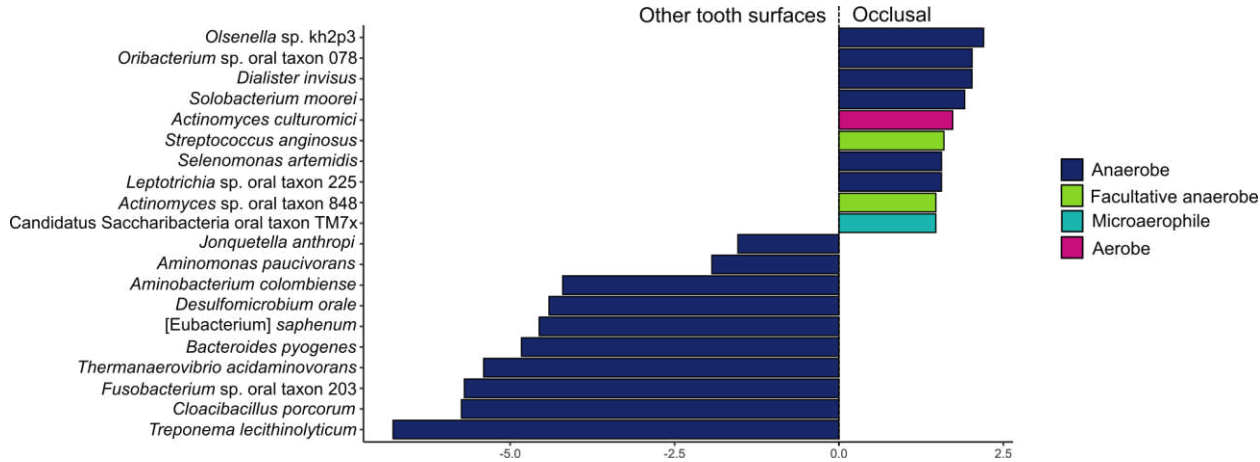
437 *Postmortem environmental colonization*

438 Whether contamination by infiltration of environmental microbes from the burial context is introduced in a  
439 non-random way across the oral cavity is not known. Because different properties of calculus across the  
440 dentition could make certain regions more susceptible to external colonization, we investigated the  
441 distribution of environmental contaminant reads in our samples. On species level, a total of 215 taxa (out  
442 of 556 taxa) were identified as putative environmental contaminants in the entire dataset, using the bone  
443 samples from the mandibles as a proxy for colonizing microbes from the burial ground. This analysis was  
444 performed at the species level, as it is possible for taxa in the same genus to grow in different habitats.  
445 We tested whether the distribution of these species across the dentition was influenced by tooth surface,  
446 tooth position, jawbone or deposit mass using linear mixed effects modeling; however, we found that  
447 none of these factors outperformed the null model. Therefore, it appears that contamination is randomly  
448 distributed across the dental arcade (LME, individual as random effect; Figure 6B).

449 *Occlusal calculus*

450 The occlusal dental calculus analyzed in this study differed from the calculus from other tooth surfaces in  
451 several ways, and was therefore excluded from most analyses. During sampling, occlusal calculus was  
452 found to have a different consistency from the other calculus, being less dense and having less structural  
453 integrity. Occlusal calculus was found to have a higher amount of DNA damage than other calculus. For  
454 reads mapping to *Tannerella forsythia*, a model including tooth surface and deposit mass best predicted  
455 damage at the 1st base at the 5' end of the fragment (LME, individual as random effect,  $p=0.018$ ), with  
456 occlusal samples having higher levels of damage than other samples (Figure S4). Further, occlusal  
457 calculus samples broke the assumption of homogeneity of dispersion for the community composition,  
458 which may be due to the fact that they were only collected from a single individual, and from only  
459 posterior teeth on the same side of the mouth. Overall, we found that despite forming on posterior teeth,

460 occlusal calculus samples are somewhat enriched in aerotolerant species, possibly due to their more  
461 exposed location on the tooth, compared to the lingual and labial surfaces of the posterior teeth that  
462 directly abut the tongue and buccal mucosa, respectively (Figure 8).

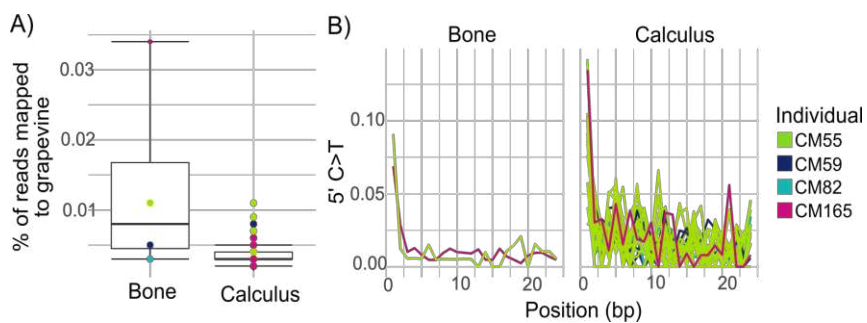


463

464 **Figure 8. Differential abundance of taxa in occlusal samples compared to others.** Only the top ten  
465 taxa are shown, and the bars are coloured by aerotolerance of the taxa.

466 *Plant DNA*

467 Ancient dental calculus is a potentially valuable source of information about ancient diets, as it is possible  
468 to directly study diet-related biomolecules and microfossils incorporated in the calculus during an  
469 individual's lifetime. Researchers have previously attempted to identify dietary sources using DNA from  
470 dental calculus (Warinner *et al.* 2014; Weyrich *et al.* 2017), an approach that also has many difficulties  
471 due to the exceptionally low number of dietary DNA sequences typically found in dental calculus (Mann *et*  
472 *al.* 2020). The dental calculus samples in this study contained trace amounts of plant DNA fragments  
473 (between 170-1578 reads per individual, or 0.002-0.011% of total reads) mapping to the grapevine (*Vitis*  
474 *vinifera*) genome, which is currently and historically widely cultivated in the region. However, it was  
475 noticed that similar numbers of grapevine reads (205-2119 reads, or 0.003-0.034%) were also recovered  
476 in the mandibular bone control samples (Figure 7A). Both sets of reads were found to have C to T  
477 damage typical of ancient DNA (7-9% for bones and 3-14% for calculus; Figure 7B), but at lower levels  
478 than observed for the oral bacterium *T. forsythia* (11-21%; Figure 2B). The presence of grapevine reads  
479 in both dental calculus and bone, together with the lower amount of damage, suggests a likely  
480 postmortem origin of the grapevine DNA. However, a dietary origin of the grapevine DNA cannot  
481 completely be excluded, as a wild variety has been documented in the region since the Palaeolithic (Aura  
482 *et al.* 2005; Iriarte-Chiapusso *et al.* 2017).



483

484 **Figure 7. Presence of grapevine DNA in bones and dental calculus samples.** A) The percentage of  
485 reads that aligned to the grapevine genome per sample. B) C to T miscoding lesions at the 5' end of the  
486 read, for each sample with >500 reads aligning to grapevine.

487

488 **Discussion**

489 A potentially uneven distribution of microbes in microbiomes can cause biases in downstream analyses if  
490 spatial variation is not taken into account during sampling design and data interpretation. Archaeological  
491 dental calculus provides a valuable window into the evolution of the oral microbiome, but to date it has not  
492 been clear to what degree microbial taxa are spatially patterned across the dentition and, thus, to what  
493 degree sampling strategy might impact comparative studies of dental calculus microbial communities. The  
494 results of present-day dental plaque studies cannot be directly applied to dental calculus because the two  
495 substrates reflect different levels of biofilm maturity and have slightly different composition (Velsko *et al.*  
496 2019), and in previous studies of spatial variation in archaeological dental calculus, which sampled  
497 diverse individual teeth from a large number of individuals (Farrer *et al.* 2018), potentially confounding  
498 factors such as individual, temporal, environmental, and taphonomic differences were not controlled for.  
499 Here, we have presented a systematic study of intra-individual variation in archaeological dental calculus  
500 by focusing on intensive, comprehensive sampling of the dentitions of four contemporaneous individuals  
501 from the same burial context.

502 Overall, we find that although there are small differences in the spatial distribution of anaerobic and  
503 aerotolerant taxa, as well as minor associations between taxonomic composition and initial calculus  
504 deposit size, these factors account for very little of the overall microbial and functional variation within  
505 dental calculus. Spatial patterns in the oral microbiome that have been identified in studies of modern  
506 dental plaque (Haffajee *et al.* 2009; Simon-Soro and Tomás 2013; Proctor *et al.* 2018) are not obvious in  
507 this study. Such patterns may have been present during life but were subsequently lost over time due to  
508 taphonomy, or these patterns may simply not be present in calculus. Although taphonomic processes,  
509 such as C to T damage accumulation and DNA fragmentation, as well as postmortem colonization of the  
510 body by environmental taxa, may obscure oral microbiome spatial patterns, we did not find these factors  
511 to correlate with the microbial patterns we observed. A study of modern dental calculus that investigates  
512 species spatial patterning will be needed to determine if the patterns observed in dental plaque are  
513 maintained as the biofilm matures and calcifies into dental calculus.

514 Although this study investigated a small number of individuals from a single archaeological site, the  
515 purpose of this study design was to limit the number of potentially confounding factors, such as different  
516 sample ages, different burial conditions, and different storage and handling practices after excavation.  
517 Microbial spatial patterning may differ in other populations or at other archaeological sites, and this  
518 warrants further investigation. However, as the species profiles of human dental calculus appear to be  
519 more consistent across time, space, and health status than dental plaque (Velsko *et al.* 2019; Fellows  
520 Yates *et al.* 2021), it is possible that any variation will be very minor.

521 Although we observed few spatial patterns in archaeological dental calculus, we find that occlusal  
522 calculus may represent a special exception. Dental calculus rarely accumulates on the occlusal surfaces  
523 of teeth, in part due to the abrasive forces of mastication, and large deposits of occlusal calculus are  
524 generally indicative of physiological injury or dysfunction. Here, only one individual had occlusal calculus,  
525 but this calculus had a distinct texture, higher DNA damage, and different levels of taxonomic dispersion  
526 compared to other dental calculus in the study, even from the same individual. Although further research

527 on a larger number of individuals is necessary, occlusal calculus is likely not representative of oral  
528 microbiome communities, and therefore should be avoided in comparative studies of microbial variation  
529 across individuals.

530 Beyond microbes, dental calculus is also valuable because it entraps dietary and other environmental  
531 debris during life, and thus can provide clues about the foods and activities of past societies (Hardy *et al.*  
532 2009; Leonard *et al.* 2015; Power *et al.* 2015; Radini *et al.* 2017). Although dietary proteins have been  
533 shown to preserve within dental calculus (Hendy *et al.* 2018; Wilkin *et al.* 2020; Scott *et al.* 2021), the  
534 metagenomic recovery of dietary DNA from calculus has yielded more equivocal results (Mann *et al.*  
535 2020). The recovery and authentication of eukaryotic DNA in metagenomic datasets is not trivial due to  
536 complicating factors such as the very low number of non-host eukaryotic DNA fragments typically found in  
537 dental calculus and the problem of microbial contamination in eukaryotic reference genomes, which can  
538 lead to false positives (Mann *et al.* 2020). Here, we show that an additional complicating factor may be  
539 contamination from the environment, and specifically from nearby agricultural fields. It is therefore  
540 advisable to include environmental controls, such as bone or sediment samples, in metagenomic studies  
541 of diet. Another authentication aid may be the use of complementary dietary identification methods, such  
542 as microfossil analysis or palaeoproteomics. Through proteomic analyses, for example, it is possible to  
543 deduce the part of an organism from which the biomolecules originate, such as seed proteins from plant  
544 seeds, or milk proteins from dairy products. Combining methods may thus aid researchers in establishing  
545 the plausibility of a given organism being incorporated into dental calculus as a food as opposed to  
546 environmental contamination.

547 To conclude, we find that in most applications a single sample of archaeological dental calculus can be  
548 used to represent an individual in comparative studies of the ancient oral microbiome. The use of a single  
549 sample instead of multiple samples, either pooled or studied separately, reduces the destructive demands  
550 on this finite archaeological material. However, as there are minor spatial patterns present, care should  
551 be taken to record the sampling location within the oral cavity for each dental calculus sample, whenever  
552 possible. This makes it possible to later reevaluate findings if systematic biases are suspected.

553

#### 554 **Accession numbers**

555 Genetic data have been deposited in the ENA under the accession PRJEB46022.

#### 556 **Acknowledgements**

557 This work was supported by the Werner Siemens Stiftung (“Paleobiotechnology” to C.W.), the European  
558 Research Council (STG-677576 “HARVEST” to A.G.H.), the Generalitat Valenciana (GV/2015/060 and  
559 CIDEVENT/2019/061 to DCSG), the Spanish government (PID2019-111207GA-I00 and EUR2020-  
560 112213 to DCSG), and the Max Planck Society. The authors thank James Fellows Yates for assistance  
561 with data analysis.

#### 562 **References**

563 Aas JA, Paster BJ, Stokes LN *et al.* Defining the normal bacterial flora of the oral cavity. *J Clin Microbiol*  
564 2005;43:5721–32.

565 Aron F, Hofman C, Fagernäs Z *et al.* Ancient DNA extraction from dental calculus v1. *protocols.io* 2020.

566 Aron F, Neumann GU, Brandt G. Half-UDG treated double-stranded ancient DNA library preparation for  
567 Illumina sequencing v1. *protocols.io* 2020.

568 Aura JE, Carrión Y, Estrelles E *et al.* Plant economy of hunter-gatherer groups at the end of the last Ice  
569 Age: plant macroremains from the cave of Santa Maira (Alacant, Spain) ca. 12000–9000 b.p. *Veg  
570 Hist Archaeobot* 2005;14:542–50.

571 Bates D, Mächler M, Bolker B *et al.* Fitting Linear Mixed-Effects Models Using lme4. *Journal of Statistical  
572 Software* 2015;67:1–48.

573 Brothwell DR. *Digging up Bones: The Excavation, Treatment and Study of Human Skeletal Remains*.  
574 London: British Museum, 1972.

575 Dabney J, Knapp M, Glocke I *et al.* Complete mitochondrial genome sequence of a Middle Pleistocene  
576 cave bear reconstructed from ultrashort DNA fragments. *Proc Natl Acad Sci U S A* 2013;110:15758–  
577 63.

578 Dabney J, Meyer M, Pääbo S. Ancient DNA damage. *Cold Spring Harb Perspect Biol* 2013;5.

579 Davis NM, Proctor DM, Holmes SP *et al.* Simple statistical identification and removal of contaminant  
580 sequences in marker-gene and metagenomics data. *Microbiome* 2018;6:226.

581 Ding T, Schloss PD. Dynamics and associations of microbial community types across the human body.  
582 *Nature* 2014;509:357–60.

583 Dobney K, Brothwell D. A method for evaluating the amount of dental calculus on teeth from  
584 archaeological sites. *J Archaeol Sci* 1987;14:343–51.

585 Eren AM, Borisby GG, Huse SM *et al.* Oligotyping analysis of the human oral microbiome. *Proc Natl Acad  
586 Sci U S A* 2014;111:E2875–84.

587 Fagernäs Z, García-Collado MI, Hendy J *et al.* A unified protocol for simultaneous extraction of DNA and  
588 proteins from archaeological dental calculus. *J Archaeol Sci* 2020;118:105135.

589 Farrer AG, Bekvalac J, Redfern R *et al.* Biological and cultural drivers of oral microbiota in Medieval and  
590 Post-Medieval London, UK. *bioRxiv* 2018;343889.

591 Fellows Yates JA, Velsko IM, Aron F *et al.* The evolution and changing ecology of the African hominid  
592 oral microbiome. *Proc Natl Acad Sci U S A* 2021;118.

593 Firke S. Janitor: Simple tools for examining and cleaning dirty data. 2018.

594 Franzosa EA, McIver LJ, Rahnavard G *et al.* Species-level functional profiling of metagenomes and  
595 metatranscriptomes. *Nat Methods* 2018;15:962–8.

596 Gevers D, Knight R, Petrosino JF *et al.* The Human Microbiome Project: a community resource for the  
597 healthy human microbiome. *PLoS Biol* 2012;10:e1001377.

598 Gloor GB, Macklaim JM, Pawlowsky-Glahn V *et al.* Microbiome Datasets Are Compositional: And This Is  
599 Not Optional. *Front Microbiol* 2017;8:2224.

600 Haber-Uriarte M, Avilés-Fernández A, Lomba-Maurandi. Estudio antropológico preliminar de los restos  
601 humanos calcolíticos del enterramiento múltiple de Camino del Molino (Carava de la Cruz, Murcia).  
602 In: D. Turbón, L. Fañanás, C. Rissoch, A. Rosa (ed.). *Biodiversidad Humana Y Evolución*. Barcelona,  
603 2011, 236–42.

604 Haffajee AD, Teles RP, Patel MR *et al.* Factors affecting human supragingival biofilm composition. II.  
605 Tooth position. *J Periodontal Res* 2009;44:520–8.

606 Hardy K, Blakeney T, Copeland L *et al.* Starch granules, dental calculus and new perspectives on ancient  
607 diet. *J Archaeol Sci* 2009;**36**:248–55.

608 Hendy J, Warinner C, Bouwman A *et al.* Proteomic evidence of dietary sources in ancient dental calculus.  
609 *Proc Biol Sci* 2018;**285**.

610 Herbig A, Maixner F, Bos KI *et al.* MALT: Fast alignment and analysis of metagenomic DNA sequence  
611 data applied to the Tyrolean Iceman. *bioRxiv* 2016:050559.

612 Huson DH, Beier S, Flade I *et al.* MEGAN Community Edition - Interactive Exploration and Analysis of  
613 Large-Scale Microbiome Sequencing Data. *PLoS Comput Biol* 2016;**12**:e1004957.

614 Iriarte-Chiapusso MJ, Ocete-Pérez CA, Hernández-Beloqui B *et al.* *Vitis vinifera* in the Iberian Peninsula:  
615 A review. *Plant Biosystems - An International Journal Dealing with all Aspects of Plant Biology*  
616 2017;**151**:245–57.

617 Jeong C, Wilkin S, Amgalantugs T *et al.* Bronze Age population dynamics and the rise of dairy  
618 pastoralism on the eastern Eurasian steppe. *Proc Natl Acad Sci U S A* 2018;**115**:E11248–55.

619 Jin Y, Yip HK. SUPRAGINGIVAL CALCULUS: FORMATION AND CONTROL. *Crit Rev Oral Biol Med*  
620 2002;**13**:426–41.

621 Kassambara A. *ggnpubr: “ggplot2” Based Publication Ready Plots*. 2018.

622 Kazarina A, Petersone-Gordina E, Kimsis J *et al.* The Postmedieval Latvian Oral Microbiome in the  
623 Context of Modern Dental Calculus and Modern Dental Plaque Microbial Profiles. *Genes* 2021;**12**.

624 Kircher M, Sawyer S, Meyer M. Double indexing overcomes inaccuracies in multiplex sequencing on the  
625 Illumina platform. *Nucleic Acids Res* 2012;**40**:e3.

626 Knights D, Kuczynski J, Charlson ES *et al.* Bayesian community-wide culture-independent microbial  
627 source tracking. *Nat Methods* 2011;**8**:761–3.

628 Kolenbrander PE. Intergeneric coaggregation among human oral bacteria and ecology of dental plaque.  
629 *Annu Rev Microbiol* 1988;**42**:627–56.

630 Kuznetsova A, Brockhoff PB, Christensen RHB. ImerTest Package: Tests in Linear Mixed Effects Models.  
631 *Journal of Statistical Software* 2017;**82**:1–26.

632 Lahti L, Shetty S. *Microbiome R Package*., 2012.

633 Leonard C, Vashro L, O’Connell JF *et al.* Plant microremains in dental calculus as a record of plant  
634 consumption: A test with Twe forager-horticulturalists. *Journal of Archaeological Science: Reports*  
635 2015;**2**:449–57.

636 Li H, Durbin R. Fast and accurate short read alignment with Burrows-Wheeler transform. *Bioinformatics*  
637 2009;**25**:1754–60.

638 Li H, Handsaker B, Wysoker A *et al.* The Sequence Alignment/Map format and SAMtools. *Bioinformatics*  
639 2009;**25**:2078–9.

640 Lomba Maurandi J, López Martínez M, Ramos Martínez F. Un excepcional sepulcro del Calcolítico:  
641 Camino del Molino (Caravaca de la Cruz). 2009:205–19.

642 Lomba Maurandi J, López Martínez M, Ramos Martínez F *et al.* El enterramiento múltiple, calcolítico, de  
643 Camino del Molino (Caravaca, Murcia). Metodología y primeros resultados de un yacimiento  
644 excepcional. *TRABAJOS DE PREHISTORIA* 2009;**66**.

645 Lüdecke D. ggeffects: Tidy Data Frames of Marginal Effects from Regression Models. *Journal of Open*  
646 *Source Software* 2018;**3**:772.

647 Mann AE, Fellows Yates JA, Fagernäs Z *et al.* Do I have something in my teeth? The trouble with genetic  
648 analyses of diet from archaeological dental calculus. *Quat Int.* 2020.

649 Mann AE, Sabin S, Ziesemer K *et al.* Differential preservation of endogenous human and microbial DNA  
650 in dental calculus and dentin. *Sci Rep* 2018;**8**:9822.

651 Mark Welch JL, Rossetti BJ, Rieken CW *et al.* Biogeography of a human oral microbiome at the micron  
652 scale. *Proc Natl Acad Sci U S A* 2016;**113**:E791–800.

653 Meyer M, Kircher M. Illumina sequencing library preparation for highly multiplexed target capture and  
654 sequencing. *Cold Spring Harb Protoc* 2010;**2010**:db.prot5448.

655 Morton JT, Marotz C, Washburne A *et al.* Establishing microbial composition measurement standards  
656 with reference frames. *Nat Commun* 2019;**10**:2719.

657 Neukamm J, Peltzer A, Nieselt K. DamageProfiler: Fast damage pattern calculation for ancient DNA. *Cold*  
658 *Spring Harbor Laboratory* 2020:2020.10.01.322206.

659 Obregon-Tito AJ, Tito RY, Metcalf J *et al.* Subsistence strategies in traditional societies distinguish gut  
660 microbiomes. *Nat Commun* 2015;**6**:6505.

661 Oh J, Byrd AL, Park M *et al.* Temporal Stability of the Human Skin Microbiome. *Cell* 2016;**165**:854–66.

662 Oksanen J, Blanchet FG, Friendly M *et al.* vegan: Community Ecology Package. 2019.

663 Ozga AT, Nieves-Colón MA, Honap TP *et al.* Successful enrichment and recovery of whole mitochondrial  
664 genomes from ancient human dental calculus. *Am J Phys Anthropol* 2016;**160**:220–8.

665 Palarea-Albaladejo J, Martín-Fernández JA. zCompositions — R package for multivariate imputation of  
666 left-censored data under a compositional approach. *Chemometrics Intellig Lab Syst* 2015;**143**:85–96.

667 Peck S, Peck L. A time for change of tooth numbering systems. *J Dent Educ* 1993;**57**:643–7.

668 Peltzer A, Jäger G, Herbig A *et al.* EAGER: efficient ancient genome reconstruction. *Genome Biol*  
669 2016;**17**:60.

670 Power RC, Salazar-García DC, Wittig RM *et al.* Assessing use and suitability of scanning electron  
671 microscopy in the analysis of micro remains in dental calculus. *J Archaeol Sci* 2014;**49**:160–9.

672 Power RC, Salazar-García DC, Wittig RM *et al.* Dental calculus evidence of Taï Forest Chimpanzee plant  
673 consumption and life history transitions. *Sci Rep* 2015;**5**:15161.

674 Proctor DM, Fukuyama JA, Loomer PM *et al.* A spatial gradient of bacterial diversity in the human oral  
675 cavity shaped by salivary flow. *Nat Commun* 2018;**9**:681.

676 Protsyuk I, Melnik AV, Nothias L-F *et al.* 3D molecular cartography using LC-MS facilitated by Optimus  
677 and 'ili software. *Nat Protoc* 2018;**13**:134–54.

678 Radini A, Nikita E, Buckley S *et al.* Beyond food: The multiple pathways for inclusion of materials into  
679 ancient dental calculus. *Am J Phys Anthropol* 2017;**162 Suppl 63**:71–83.

680 Rampelli S, Schnorr SL, Consolandi C *et al.* Metagenome Sequencing of the Hadza Hunter-Gatherer Gut  
681 Microbiota. *Curr Biol* 2015;**25**:1682–93.

682 R Core Team. R: A language and environment for statistical computing. *R Foundation for Statistical*

683 Computing, Vienna, Austria 2019.

684 Rohland N, Harney E, Mallick S *et al.* Partial uracil-DNA-glycosylase treatment for screening of ancient  
685 DNA. *Philos Trans R Soc Lond B Biol Sci* 2015;370:20130624.

686 Sankaranarayanan K, Ozga AT, Warinner C *et al.* Gut Microbiome Diversity among Cheyenne and  
687 Arapaho Individuals from Western Oklahoma. *Curr Biol* 2015;25:3161–9.

688 Schubert M, Lindgreen S, Orlando L. AdapterRemoval v2: rapid adapter trimming, identification, and read  
689 merging. *BMC Res Notes* 2016;9:88.

690 Scott A, Power RC, Altmann-Wendling V *et al.* Exotic foods reveal contact between South Asia and the  
691 Near East during the second millennium BCE. *Proc Natl Acad Sci U S A* 2021;118.

692 Simon-Soro A, Tomás I. Microbial geography of the oral cavity. *Journal of dental research* 2013.

693 Skoglund P, Northoff BH, Shunkov MV *et al.* Separating endogenous ancient DNA from modern day  
694 contamination in a Siberian Neandertal. *Proc Natl Acad Sci U S A* 2014;111:2229–34.

695 Slon V, Hopfe C, Weiβ CL *et al.* Neandertal and Denisovan DNA from Pleistocene sediments. *Science*  
696 2017;356:605–8.

697 Stahl R, Warinner C, Velsko I *et al.* Illumina double-stranded DNA dual indexing for ancient DNA v1.  
698 *protocols.io* 2019, DOI: 10.17504/protocols.io.bakticwn.

699 Utter DR, Borisy GG, Murat Eren A *et al.* Metapangenomics of the oral microbiome provides insights into  
700 habitat adaptation and cultivar diversity. 2020:2020.05.01.072496.

701 Velsko IM, Fellows Yates JA, Aron F *et al.* Microbial differences between dental plaque and historic  
702 dental calculus are related to oral biofilm maturation stage. *Microbiome* 2019;7:102.

703 Velsko IM, Warinner CG. Bioarchaeology of the human microbiome. *Bioarchaeology International*  
704 2017;1:86–99.

705 Venables WN, Ripley BD. Modern Applied Statistics with S. 2002.

706 Warinner C, Rodrigues JFM, Vyas R *et al.* Pathogens and host immunity in the ancient human oral cavity.  
707 *Nat Genet* 2014;46:336–44.

708 Warinner C, Velsko I, Fellows Yates JA. Dental calculus field-sampling protocol (warinner version) v1  
709 (*protocols.io*.7hphj5n). *protocols.io* 2019.

710 Weyrich LS, Duchene S, Soubrier J *et al.* Neanderthal behaviour, diet, and disease inferred from ancient  
711 DNA in dental calculus. *Nature* 2017;544:357–61.

712 Wickham H, Averick M, Bryan J *et al.* Welcome to the tidyverse. *Journal of Open Source Software*  
713 2019;4:1686.

714 Wickham H, Bryan J. *readxl*: Read Excel Files. 2019.

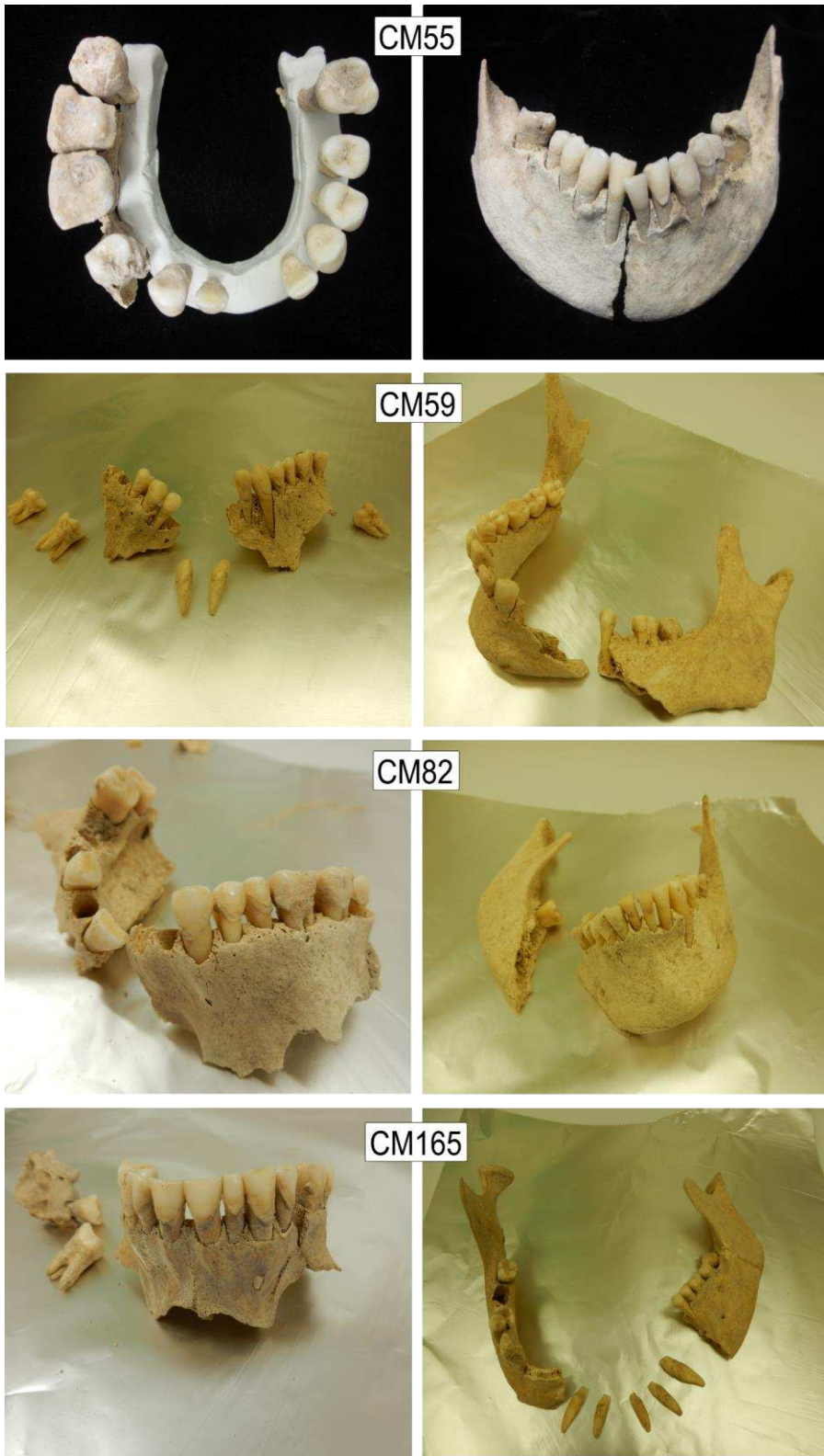
715 Wilkin S, Ventresca Miller A, Taylor WTT *et al.* Dairy pastoralism sustained Eastern Eurasian steppe  
716 populations for 5000 years. *Nature Ecology and Evolution* 2020;4:346–55.

717 Ziesemer KA, Mann AE, Sankaranarayanan K *et al.* Intrinsic challenges in ancient microbiome  
718 reconstruction using 16S rRNA gene amplification. *Sci Rep* 2015;5:16498.

719 Ziesemer KA, Ramos-Madrigal J, Mann AE *et al.* The efficacy of whole human genome capture on  
720 ancient dental calculus and dentin. *Am J Phys Anthropol* 2019;168:496–509.

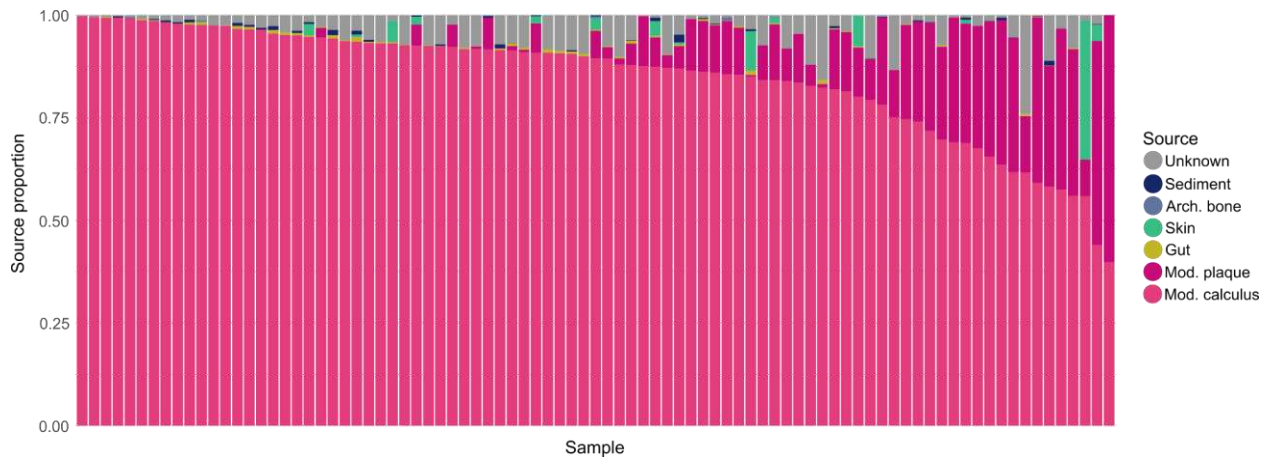
721 **Supplementary figures**

722



723

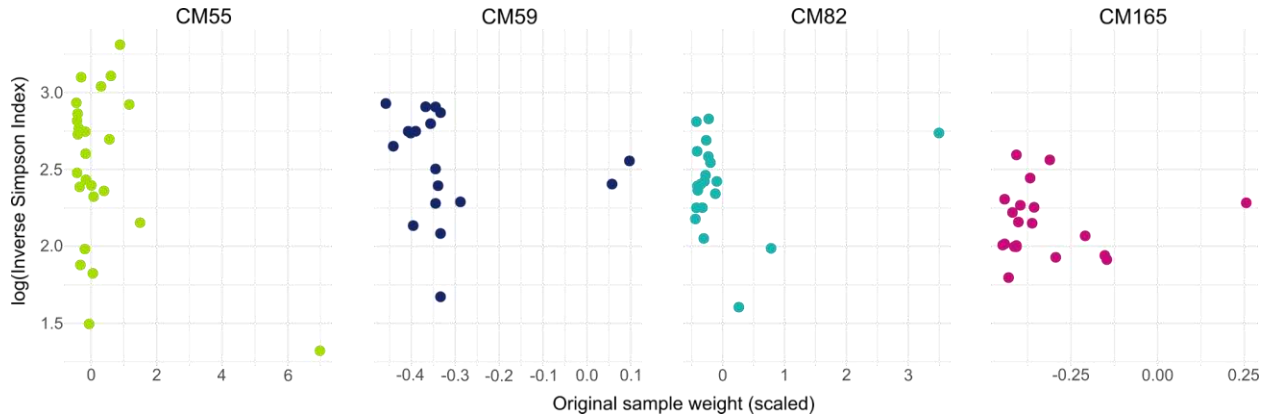
724 **S1.** Photos of the entire available dentitions of the four individuals sampled in this study.



725

726 **S2.** Sourcetracker results, generated from a genus-level OTU-table.

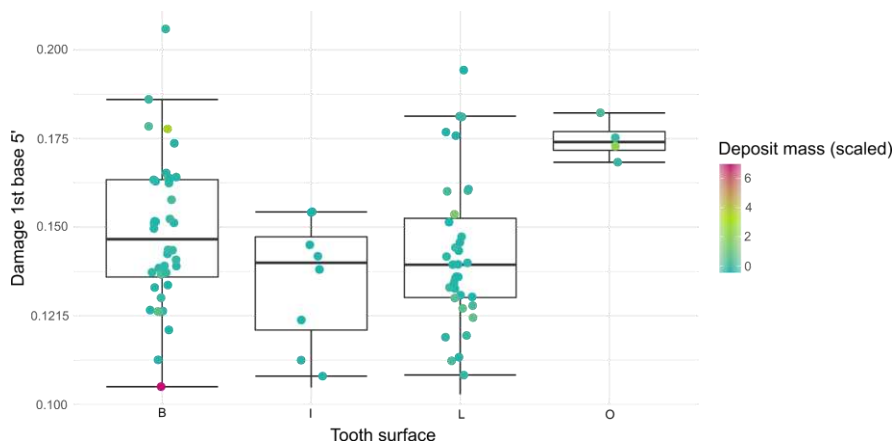
727



728

729 **S3.** Inverse Simpson Index by mass of the original calculus deposit.

730



731

732 **S4.** Damage of first base at the 5' end of fragments mapping to *Tannerella forsythia*.